

6. Hauser, M. A., Sena, D. F., Flor, J., Walter, J., Auguste, J., Larocque-Abramson, K., Graham, F., Delbono, E., Haines, J. L., Pericak-Vance, M. A., Allingham, R. R., and Wiggs, J. L. (2006) *J. Glaucoma* **15**, 358-363
7. Aung, T., Rezaie, T., Okada, K., Viswanathan, A. C., Child, A. H., Brice, G., Bhattacharya, S. S., Lehmann, O. J., Sarfarazi, M., and Hitchings, R. A. (2005) *Invest. Ophthalmol. Vis. Sci.* **46**, 2816-2822
8. Maruyama, H., Morino, H., Ito, H., Izumi, Y., Kato, H., Watanabe, Y., Kinoshita, Y., Kamada, M., Nodera, H., Suzuki, H., Komure, O., Matsuura, S., Kobatake, K., Morimoto, N., Abe, K., Suzuki, N., Aoki, M., Kawata, A., Hirai, T., Kato, T., Ogasawara, K., Hirano, A., Takumi, T., Kusaka, H., Hagiwara, K., Kaji, R., and Kawakami, H. (2010) *Nature* **465**, 223-226
9. Albagha, O. M. E., Visconti, M. R., Alonso, N., Langston, A. L., Cundy, T., Dargie, R., Dunlop, M. G., Fraser, W. D., Hooper, M. J., Isaia, G., Nicholson, G. C., del Pino Montes, J., Gonzalez-Sarmiento, R., di Stefano, M., Tenesa, A., Walsh, J. P., and Ralston, S. H. (2010) *Nat. Genet.* **42**, 520-524
10. Li, Y., Kang, J., and Horwitz, M. S. (1998) *Mol. Cell. Biol.* **18**, 1601-1610
11. Rezaie, T., and Sarfarazi, M. (2005) *Genomics* **85**, 131-138
12. Kroeber, M., Ohlmann, A., Russell, P., and Tamm, E. R. (2006) *Exp. Eye Res.* **82**, 1075-1085
13. De Marco, N., Buono, M., Troise, F., and Diez-Roux, G. (2006) *J. Biol. Chem.* **281**, 16147-16156
14. Schwamborn, K., Weil, R., Courtois, G., Whiteside, S. T., and Israel, A. (2000) *J. Biol. Chem.* **275**, 22780-22789
15. Sudhakar, C., Nagabhushana, A., Jain, N., and Swarup, G. (2009) *PLoS ONE* **4**, e9114
16. Zhu, G., Wu, C. J., Zhao, Y., and Ashwell, J. D. (2007) *Curr. Biol.* **17**, 1438-1443
17. Ying, H., Shen, X., Park, B. C., and Yue, B. Y. J. T. (2010) *PLoS One* **5**, e9168
18. Park, B. C., Shen, X., Samaraweera, M., and Yue, B. Y. J. T. (2006) *Am. J. Pathol.* **169**, 1976-1989
19. Glickman, M. H., and Ciechanover, A. (2002) *Physiol. Rev.* **82**, 373-428
20. McCray, B. A., and Taylor, J. P. (2008) *Neurosignals* **16**, 75-84
21. Kirkin, V., McEwan, D. G., Novak, I., and Dikic, I. (2009) *Mol. Cell* **34**, 259-269
22. Mukhopadhyay, D., and Riexman, H. (2007) *Science* **315**, 201-205
23. Mizushima, N. (2007) *Genes Dev.* **21**, 2861-2873
24. Meijer, A. J., and Codogno, P. (2009) *Crit. Rev. Clin. Lab. Sci.* **46**, 210-240
25. Eskelinen, E. (2005) *Autophagy* **1**, 1-10
26. Bao, X. H., Naomoto, Y., Hao, H. F., Watanabe, N., Sakurama, K., Noma, K., Motoki, T., Tomono, Y., Fukazawa, T., Shirakawa, Y., Yamatsuji, T., Matsuoka, J., and Takaoka, M. (2010) *Int. J. Mol. Med.* **25**, 493-503
27. Mizushima, N., Yoshimori, T., and Levine, B. (2010) *Cell* **140**, 313-326
28. Levine, B., and Kroeme, G. (2008) *Cell* **732**, 27-42
29. Mizushima, N., Levine, B., Cuervo, M., and Kilonsky, D. J. (2008) *Nature* **451**, 1069-1075
30. Rubinsztein, D. C. (2006) *Nature* **443**, 780-786
31. Krishnamoorthy, R. R., Agarwal, P., Prasanna, G., Vopat, K., Lambert, W., Sheedlo, H. J., Pang, I. H., Shade, D., Wordinger, R. J., Yorio, T., Clark, A. F., and Agarwal, N. (2001) *Brain Res. Mol. Brain Res.* **86**, 1-12
32. Van Bergen, N. J., Wood, J. P., Chidlow, G., Trounce, I. A., Casson, R. J., Ju, W. K., Weinreb, R. N., and Crowston, J. (2009) *Invest. Ophthalmol. Vis. Sci.* **50**, 4267-4272
33. Greene, L. A., Tischler, A. S. (1976) *Proc. Natl. Acad. Sci. USA* **73**, 2424-2428
34. Choi, J., Miller, A. M., Nolan, M. J., Yue, B. Y., Thotz, S. T., Clark, A. F., Agarwal, N., and Knepper, P. A. (2005) *Invest. Ophthalmol. Vis. Sci.* **46**, 214-222
35. Park, B. C., Tibudan, M., Samaraweera, M., Shen, X., and Yue, B. Y. J. T. (2007) *Genes Cells* **12**, 969-979
36. Vittitow, J. L., and Borrás, T. (2002) *Biochem. Biophys. Res. Commun.* **298**, 67-74

37. Caballero, M., Liton, P. B., Challa, P., Epstein, D. L., and Gonzalez, P. (2004) *Biochem. Biophys. Res. Commun.* **323**, 1048-1054
38. Bence, N. F., Sampat, R. M., and Kopito, R. R. (2001) *Science* **292**, 1552-1555
39. Bence, N. F., Bennet, E. J., and Kopito, R. R. (2005) *Methods Enzymol.* **399**, 481-490
40. Koga T., Shen, X., Qiu Y, Park BC, Shyam R, and Yue, B. Y. J. T. (2010) *Am. J. Pathol.* **176**, 343-352
41. Chi, Z. L., Akahori, M., Obazawa, M., Minami, M., Noda, T., Nakaya, N., Tomarev, S., Kawase, K., Yamamoto, T., Noda, S., Sasaoka, M., Shimazaki, A., Takada, Y., Iwata, T. (2010) *Hum. Mol. Genet.* **19**, 2606-2615
42. Huang, Y., Li, Z., van Rooijen, N., Wang, N., Pang, C. P., and Cui, Q. (2007) *Exp. Eye Res.* **85**, 659-666
43. Eskelinen, E.-L. (2008) *Autophagy* **4**, 257-260
44. Martinez-Vicente, M., Talloczy, Z., Wong, E., Tang, G., Koga, H., Kaushik, S., de Vries, R., Arias, E., Harris, S., Sulzer, D., and Cuervo, A. M. (2010) *Nat. Neurosci.* **13**, 567-576
45. Klinosky, D. J., Cuervo, A. M., and Seglen, P. O. (2007) *Autophagy* **3**, 181-206
46. Mizushima, N., and Yoshimori, T. (2007) *Autophagy* **3**, 542-545
47. Webb, J. L., Ravikumar, B., Atkins, J., Skepper, J. N., and Rubinsztein, D. C. (2003) *J. Biol. Chem.* **278**, 25009-25013
48. Pan, T., Kondo, S., Le, W., and Jankovic, J. (2008) *Brain* **131**, 1969-1978
49. Bence, N. F., Sampat, R. M., and Kopito, R. R. (2001) *Science* **292**, 1552-1555
50. Mayer, R. J. (2003) *Drugs News Perspect.* **16**, 103-108
51. Ross, C. A., and Pickart, C. M. (2004) *Trends Cell Biol.* **14**, 703-711
52. McKinnon, S. J. (2003) *Front Biosci.* **8**, s1140-1156
53. Gupta, N., and Yucel, Y. H. (2007) *Curr. Opin. Ophthalmol.* **18**, 110-114
54. Normando, E. M., Coxon, K. M., Guo, L., and Cordeiro, M. F. (2009) *Exp. Eye Res.* **89**, 446-447
55. Garcia-Arencibia, M., Hochfeld, W. E., Toh, P. P. C., and Rubinsztein, D. C. (2010) *Semin. Cell Dev. Biol.* **21**, 691-698
56. Glick, D., Barth, S., and Macleod, K. F. (2010) *J. Pathol.* **221**, 3-12
57. Hara, T., Nakamura, K., Matsui, M., Yamamoto, A., Nakahara, Y., Suzuki-Migishima, R., Yokoyama, M., Mishima, K., Saito, I., Okano, H., and Mizushima, N. (2006) *Nature* **441**, 885-889
58. Spencer, B., Potkar, R., Trejo, M., Rockenstein, E., Patriek, C., Gindi, R., Adame, A., Wyss-Coray, T., and Masliah, E. (2009) *J. Neurosci.* **29**, 13578-13588
59. Cherra, S. J., Dagda, R. K., and Chu, C. T. (2010) *Neuropathol. Applied Neurobiol.* **36**, 125-132
60. Jana, N. R., Zemskov, E. A., Wang, G., and Nukina, N. (2001) *Hum. Mol. Genet.* **10**, 1049-1059
61. Matsuda, N., and Tanaka, K. (2010) *J. Alzheimer's Dis.* **19**, 1-9
62. Knoflerle, J., Koch, J. C., Ostendorf, T., Michel, U., Planchamp, V., Vutova, P., Tonges, L., Stadelmann, C., Bruck, W., Bahr, M., and Lingor, P. (2010) *Proc. Natl. Acad. Sci.* **107**, 6064-6069
63. Ralston, S. H. (2008) *Bone* **43**, 819-825
64. Wong, E., and Cuervo, A. M. (2010) *Nat. Neurosci.* **13**, 805-811
65. Park, B. C., Ying, H., Shen, X., Park, J. S., Qiu, Y., Shyam, R., and Yue, B. Y. J. T. (2010) *PLoS One* **5**, e11547
66. Tezel, G. (2008) *Prog. Brain Res.* **173**, 409-421
67. Sarkar, S., Krishna, G., Imarisio, S., Saiki, S., O'Kane, C. J., and Rubinsztein, D. C. (2008) *Hum. Mol. Genet.* **17**, 170-178
68. Renna, M., Jimenez-Sanchez, M., Sarkar, S., and Rubinsztein, D. C. (2010) *J. Biol. Chem.* **285**, 11061-11067

FOOTNOTES

* We thank Ruth Zelkha for expert imaging and Jack Gibbons, Division of Biological Sciences for immunogold electron microscopy. This work was supported by National Eye Institute, National Institutes of Health, Grants EY018828, EY005628, EY003890 (to B.Y.J.T.Y.), and Core Grant EY01792, and the Ministry of Health, Labor, and Welfare, and the Ministry of Education, Culture, Sports, Science and Technology of Japan (to T.I.). The costs of publication of this article were defrayed in part by the payment of page charges.

The abbreviations used are: ALS, amyotrophic lateral sclerosis; Atg5, autophagy-related gene 5; NH_4Cl , ammonium chloride; DAPI, 4',6-diamidino-2-phenylindole; DMSO, dimethylsulfoxide; DOX, doxycycline; GAPDH, glyceraldehyde 3-phosphate dehydrogenase; E50K, Glu50Lys; Epoxo, epoxomicin; GFP, green fluorescence protein; H & E, hematoxylin and eosin; His, histidine; $\text{IFN-}\gamma$, interferon- γ ; IB, immunoblotting; IP, immunoprecipitation; kb, kilobases; kDa, kilodaltons; LC3, microtubule-associated protein 1 light chain 3; LCT, lactacystin; 3-MA, 3-methyladenine; NC, negative control; NEMO, NF- κB essential modulator; NTG, normal tension glaucoma; OPTN, optineurin; PCR, polymerase chain reaction; PI3K, phosphatidylinositol 3-kinase; POAG, primary open angle glaucoma; PSMB5, proteasome regulatory $\beta 5$ subunit; RGC, retinal ganglion cell; RPE cell, retinal pigment epithelial cell; Rapa, rapamycin; SDS-PAGE, sodium dodecyl sulfate-polyacrylamide gel electrophoresis; TNF- α , tumor necrosis factor- α ; TUNEL, terminal deoxynucleotidyl transferase dUTP nick end labeling; WT, wild type.

FIGURE LEGENDS

Fig. 1. Effects of proteasomal, autophagic, and lysosomal inhibitors on levels of the endogenous optineurin (OPTN) in RGC5 (A) and PC12 (B) cells. Cells were treated for 16 h with vehicle DMSO or H_2O , or proteasomal (lactacystin [LCT] and epoxomicin [Epoxo]), autophagic (3-MA), or lysosomal (NH_4Cl) inhibitors. In a separate experiment, cells were also treated with rapamycin (Rapa) or vehicle (H_2O) for 16 h. Proteins (25 μg) in cell lysates were immunoblotted with anti-optineurin or anti-glyceraldehyde 3-phosphate dehydrogenase (GAPDH). Densitometry was performed. The optineurin/GAPDH relative to the DMSO or H_2O control ratios are presented.

Fig. 2. A. Total lysates from RGC5 cells without or with treatment of lactacystin (LCT, 1 μM , 16 h) were immunoblotted (IB) with polyclonal anti-optineurin (anti-OPTN, left panel), anti-GAPDH, or monoclonal anti-ubiquitin (anti-Ub, right panel). B. Total lysates from RGC5 cells without or with the LCT treatment were immunoprecipitated (IP) with rabbit anti-OPTN polyclonal antibody or normal rabbit IgG (as a negative control, NC) followed by immunoblotting (IB) with mouse anti-Ub monoclonal antibody. Optineurin pull down by rabbit anti-OPTN, but not the rabbit IgG control, showed multiple bands immunoreactive to anti-Ub (left panel). The intensity of the ubiquitin-positive bands was enhanced by prior LCT treatment. The same blot was also probed with anti-OPTN (right panel) to verify the IP procedure. *, the 74-kDa optineurin band.

Fig. 3. Foci formation in RGC5 (A) and PC12 (B) cells after 20 h-transfection with pEGFP-N1 (mock control), pOPTN_{WT}-GFP, and pOPTN_{E50K}-GFP to express GFP, wild type and E50K optineurin-GFP. The optineurin-GFP fusion proteins distributed diffusely in the cytoplasm of RGC5 and PC12 cells with dots or granular structures (arrows) observed most notably near the nucleus. These structures are referred to as foci. Scale bar, 10 μm .

Fig. 4. A. PSMB5 immunostaining (in red) in RGC5 cells. The cells were transfected for 20 h to express GFP, OPTN_{WT}-GFP, or OPTN_{E50K}-GFP. All transfectants displayed green fluorescence. Note a

reduced PSMB5 staining intensity in optineurin-GFP-expressing green cells compared with GFP-expressing or non-transfected cells. The reduction was more striking with the E50K mutation than the wild type. Scale bar, 10 μ m. **B.** Western blotting for PSMB5 protein level. RGC5 cells were transfected for 20 h with pTarget, pTarget-OPTN_{WT}, or pTarget-OPTN_{E50K}. Total lysate was subject to SDS-PAGE and immunoblotting (IB) using polyclonal rabbit anti-optineurin, anti-PSMB5 or anti-GAPDH. The optineurin (OPTN) level, normalized to that of GAPDH, was increased by 9.8 and 7.5 fold, respectively, after wild type and E50K optineurin-GFP transfection. The PSMB5/GAPDH relative to the GFP control ratios are presented. Similar results were also obtained with PC12 cells (data not shown). **C.** GFP^u reporter assay. RGC5 cells were co-transfected with GFP^u and pDsRed, pOPTN_{WT}-DsRed, or pOPTN_{E50K}-DsRed for 20 h. The transfected cells displaying both green and red fluorescence were examined by confocal sequential analyses. The loss of GFP^u green fluorescence is an indication of proteasome activity. The fluorescence intensity from GFP^u is thus inversely correlated to the proteasome activity. Scale bar, 10 μ m. **D.** The intensity of green fluorescence from GFP^u in red fluorescent transfected cells was quantified. Results are presented as mean \pm SEM (n \geq 60) per transfected cells. The higher the value, the lower is the proteasome activity. *, P < 0.0001 compared to DsRed controls.

Fig. 5. **A.** LC3 immunostaining in transfected RGC5 cells. The cells transfected for 20 h to express GFP, OPTN_{WT}-GFP, or OPTN_{E50K}-GFP were stained with rabbit anti-LC3 in red. The GFP and LC3 merged images are presented. Note an increased LC3 staining in optineurin transfected green cells. The optineurin foci (green) and LC3 (red) were colocalized partially in the perinuclear region in yellow. Bar, 10 μ m. **B.** Western blotting for LC3 protein level. RGC5 cells were transfected for 20 h with pTarget, pTarget-OPTN_{WT}, or pTarget-OPTN_{E50K}. Total lysate was subject to SDS-PAGE and immunoblotting (IB) using rabbit anti-optineurin, mouse anti-LC3 or rabbit anti-GAPDH. Both LC3-I and LC3-II protein bands were detected. The optineurin (OPTN) level, normalized to that of GAPDH, was increased by 11.5 and 12.3 fold respectively after wild type and E50K optineurin transfection. The LC3/GAPDH relative to the pTarget control ratios are presented. Similar alterations were also observed in PC12 cells (data not shown).

Fig. 6. **A.** Optineurin and PSMB5 immunostaining in RGC5 cells. The cells were treated with TNF- α (100 ng/ml) or IFN- γ (20 ng/ml) for 24 h and were stained with polyclonal rabbit anti-optineurin in green or polyclonal rabbit anti-PSMB5 in red. The micrographs shown for optineurin and PSMB5 staining were from different specimens. **B.** Optineurin and PSMB5 immunostaining in RGC5 cells. The cells were treated with TNF- α or IFN- γ as in **A.** The specimens were double stained with rabbit anti-optineurin in green and monoclonal anti-LC3 in red. Cells from the same fields are shown for both optineurin and LC3 staining. Scale bar, 10 μ m. **C.** Immunoblotting (IB) using anti-optineurin (OPTN), anti-PSMB5, anti-LC3, and anti-GAPDH in cells untreated (lane 1, control), or treated with TNF- α (lane 2) or IFN- γ (lane 3) for 24 h. Note that the 18-kDa LC3-I band was barely visible. Only the 16-kDa LC3-II band is shown. As stated earlier, LC3 exists in two forms. LC3-I is cytosolic and LC3-II is lipidated and membrane bound. The amount of LC3-II is correlated with the extent of autophagosome formation and an increasing level of LC3-II on immunoblots signals autophagy induction. Bar graph depicts the relative intensities (levels) of OPTN, PSMB5, and LC3 compared to untreated controls after normalization to the GAPDH level.

Fig. 7. **A.** Autophagosome- and autolysosome-like structures in optineurin wild type (**a** and **b**)- and E50K-GFP (**c**)-expressing RGC5 cells. By electron microscopy, the electron dense, organelle-sequestering, double- or multi-membrane structures with diameter averaged between 400-600 nm were not observed in GFP-expressing mock transfected cells (**d**). Scale bar, 5 μ m in **a**, 0.5 μ m in **b** and **c**, and 1 μ m in **d**. **B.** Autophagosome- and autolysosome-like structures are observed in inducible RGC5 cells after DOX induction to express E50K optineurin-GFP (**a-d**). A lower magnification micrograph is shown in **a** demonstrating those structures in cytoplasm of several cells. Co-localization of optineurin-GFP (25 nm gold particles) and LC3 (10 nm gold particles) in those structures is seen by immunogold labeling

experiments (c and d). The autophagosome- and autolysosome-like structures are barely detected in non-induced controls (insert in b). Scale bar, 1 μ m in a, 0.5 μ m in b, and 0.2 μ m in insert, c and d.

Fig. 8. Effects of 3-MA and rapamycin on optineurin foci formation. **A.** RGC5 cells transfected for 20 h with pOPTN_{WT}-GFP were untreated (control) or treated for 24 or 48 h with 3-MA (5 mM), an autophagy inhibitor. Optineurin foci formation was visualized under a Zeiss fluorescence microscope. Note an increased foci formation in 3-MA treated cells. **B.** RGC5 cells transfected with pOPTN_{WT}-GFP and pOPTN_{E50K}-GFP were treated for 20 h with rapamycin (2 μ M), an autophagy inducer. Note a reduction in foci formation with rapamycin treatment. Scale bar, 10 μ m. Similar results were also obtained with PC12 cells (data not shown). **C.** Percentage of caspase 3/7-positive apoptotic cells in transfected RGC5 cells. The cells transfected for 48 h to express GFP (mock control), wild type optineurin-GFP (OPTN-GFP) and E50K optineurin-GFP (E50K-GFP) were examined by a caspase 3/7 detection kit. One set of cells was treated with 2 μ M of rapamycin [(+) Rapamycin] for the last 30 h and another was untreated [(-) Rapamycin]. Images in 20 of 10 \times fields were captured and cell counting was performed to determine the total number of transfected cells (green) and the number of caspase 3/7-positive transfectants (green and red). Percentage of caspase 3/7-positive apoptotic transfected cells was calculated. Results from 3 independent experiments are shown in mean \pm SEM. *, P < 0.008 compared to GFP controls. Similar patterns were also observed with PC12 cells (data not shown).

Fig. 9. **A.** Retinal sections from 12-month-old E50K transgenic and normal littermate mice were stained with monoclonal anti-TUJ1 (in red) to highlight the RGC layer, and with hematoxylin and eosin (H & E) to demonstrate retinal layers. GCL, ganglion cell layer; IPL, inner plexiform layer; INL, inner nuclear layer; OPL, outer plexiform layer; ONL, outer nuclear layer; POS, photoreceptor outer segments; and RPE, retinal pigment epithelium. Note that the retinal thickness is reduced in E50K transgenic specimen compared to normal control. Scale bar, 50 μ m. **B.** Retinal sections from normal and E50K mice were stained in parallel with polyclonal anti-optineurin, anti-PSMB5, or anti-LC3 (all in red). All staining was done using the same antibody concentrations with identical exposure times. As RGCs are the focus of the study, staining in RGCs and the adjacent inner plexiform layer is shown in a higher magnification. Negative controls (NC) in which serial sections were stained only with secondary antibodies (for both monoclonal and polyclonal primary antibodies) are shown in inserts. There was a modest decrease in staining intensity of PSMB5 but an increase in LC3 staining in RGC layer in transgenic sections compared to normal controls. The optineurin staining was also enhanced in the transgenic mouse. Scale bar, 50 μ m. **C.** Western blotting for optineurin (OPTN), PSMB5, LC3, and GAPDH levels in retinal extracts from normal (lane 1) or E50K (lane 2) mice. Note that for LC3, the 18-kDa LC3-I band was extremely faint. Only the 16-kDa LC3-II band is shown. Bar graphs, representing results from 3 experiments, depict the levels of optineurin, PSMB5, and LC3 relative to normals after normalization to the GAPDH level. *, P < 0.0053 compared to normals. **D.** Autophagosome- and autolysosome-like structures are observed in RGCs of E50K mouse (left and middle panels), but are rarely seen in normal littermates (right panel). Bar, 1 μ m in the left panel, and 0.5 μ m in middle and right panels.

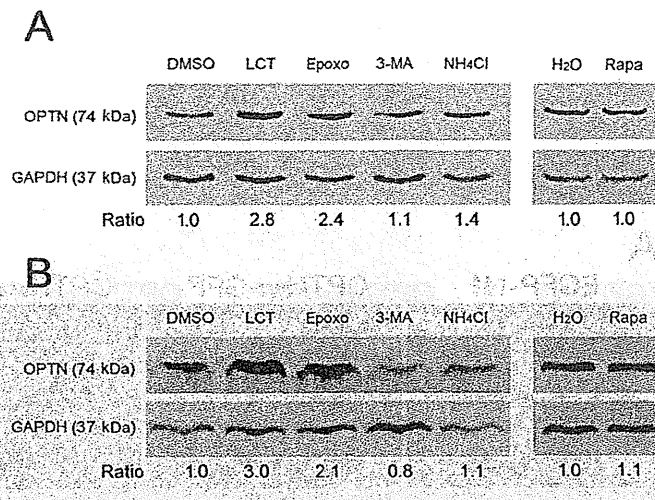


Figure 1

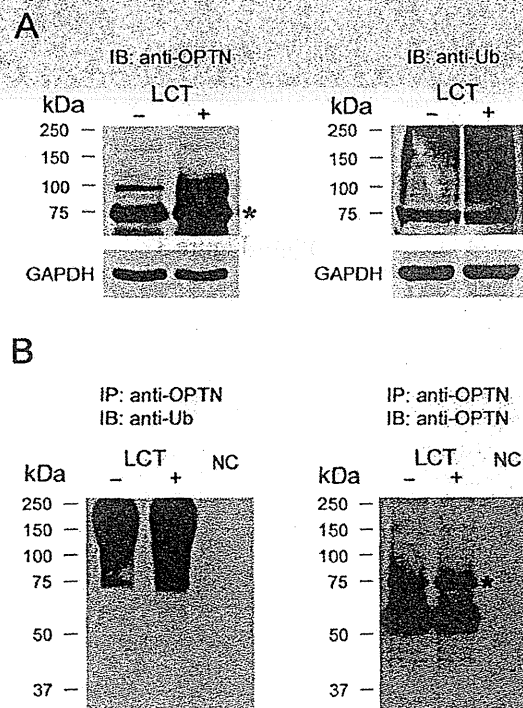


Figure 2

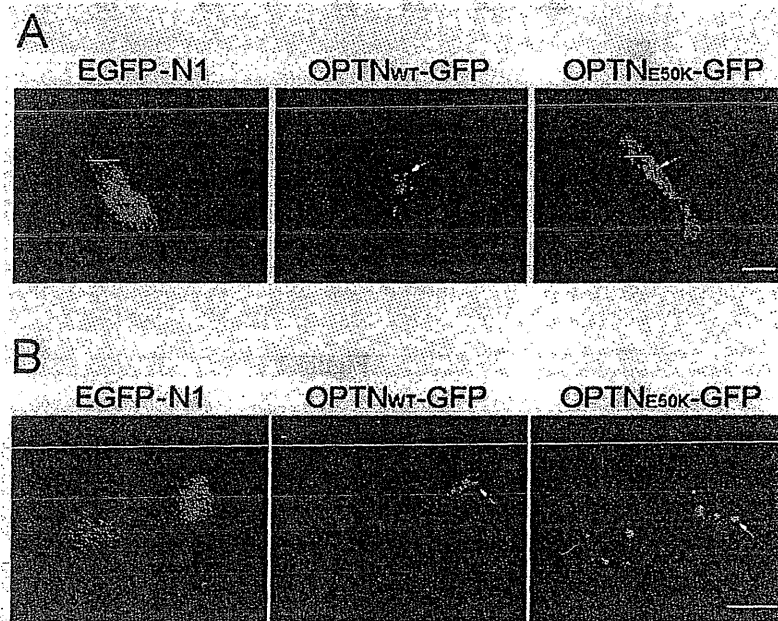


Figure 3

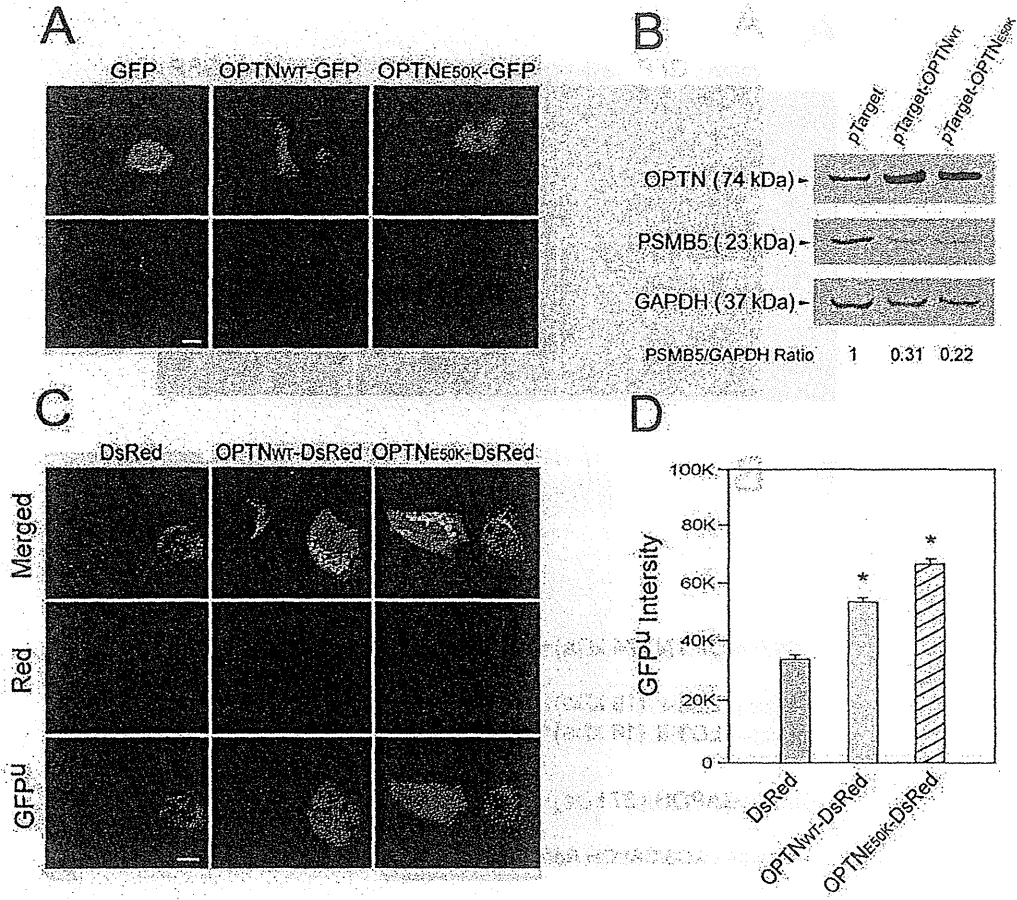


Figure 4

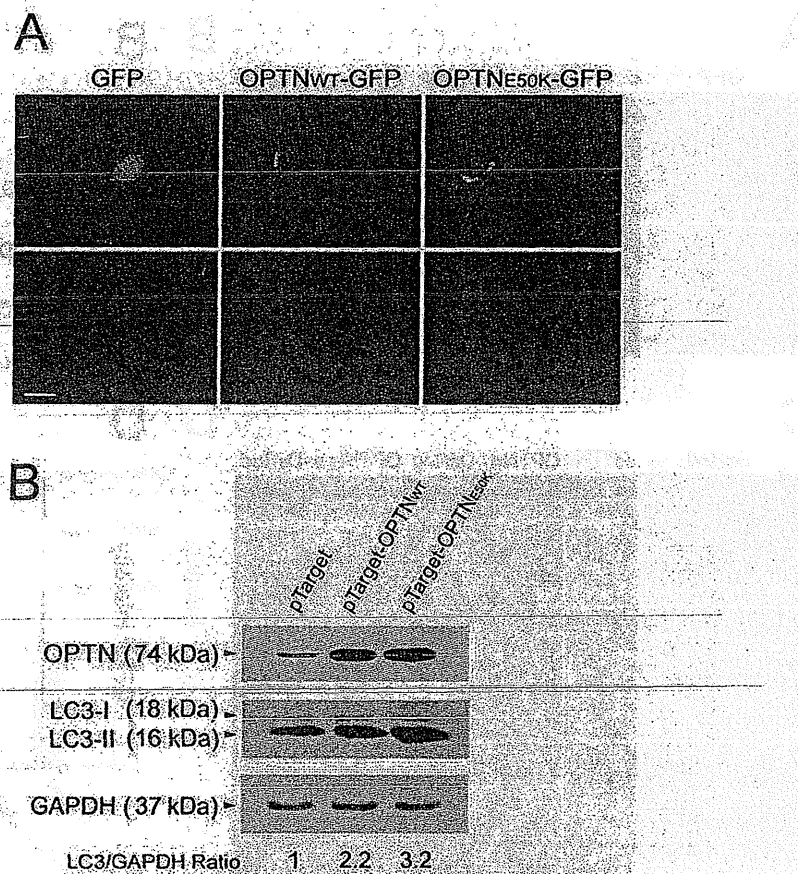


Figure 5

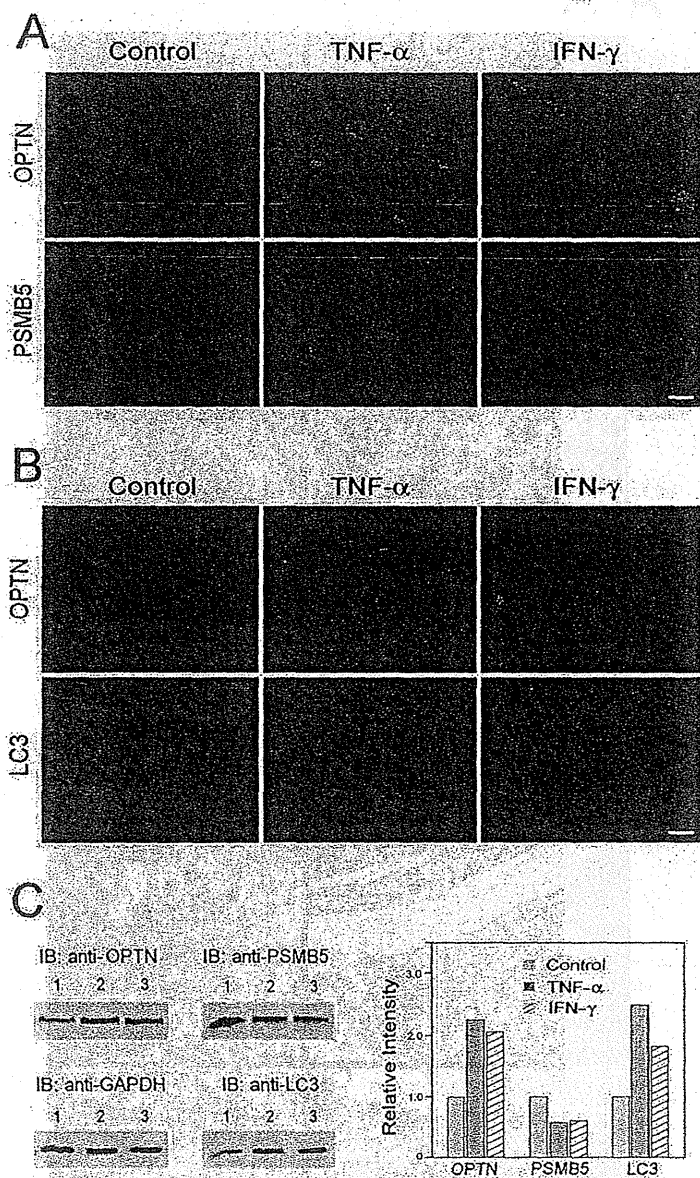


Figure 6

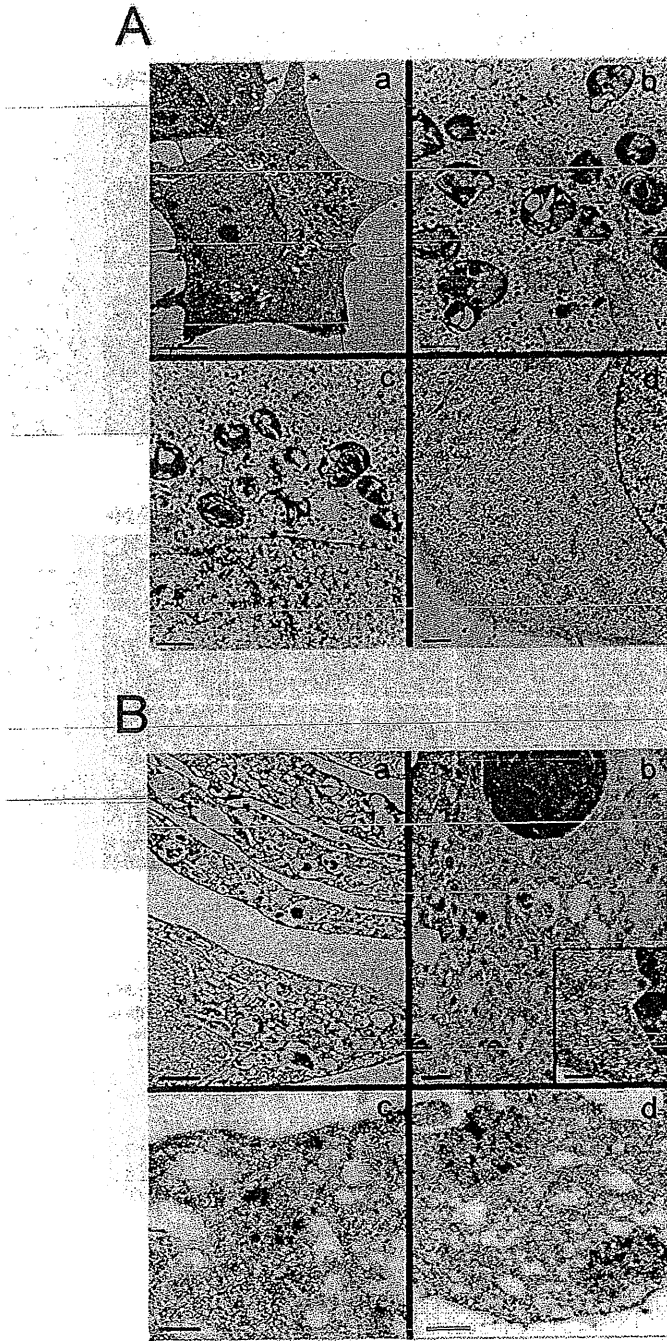


Figure 7

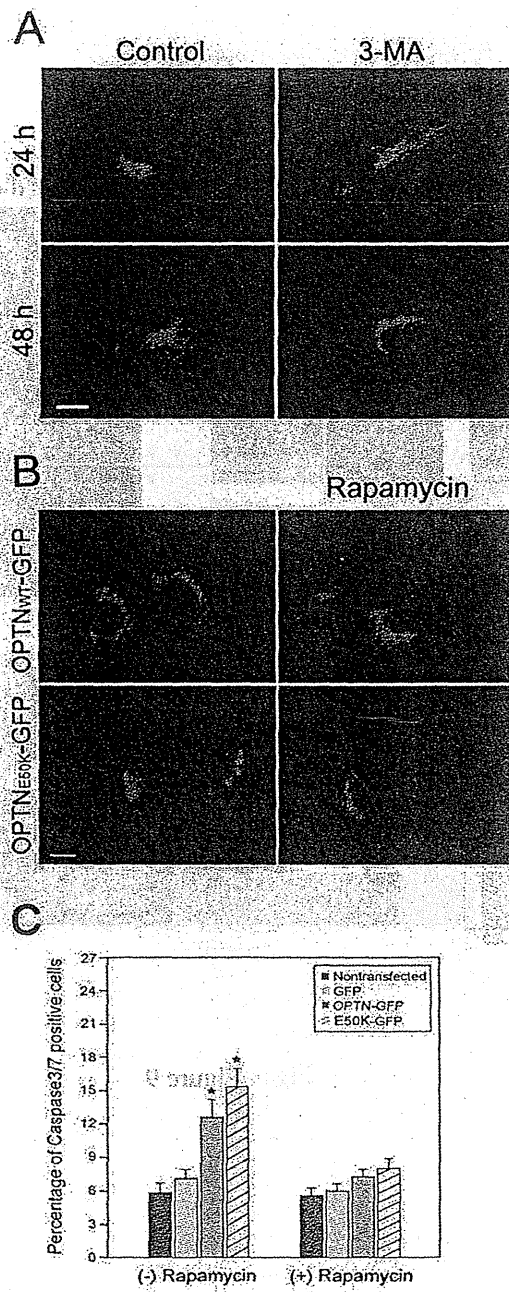


Figure 8

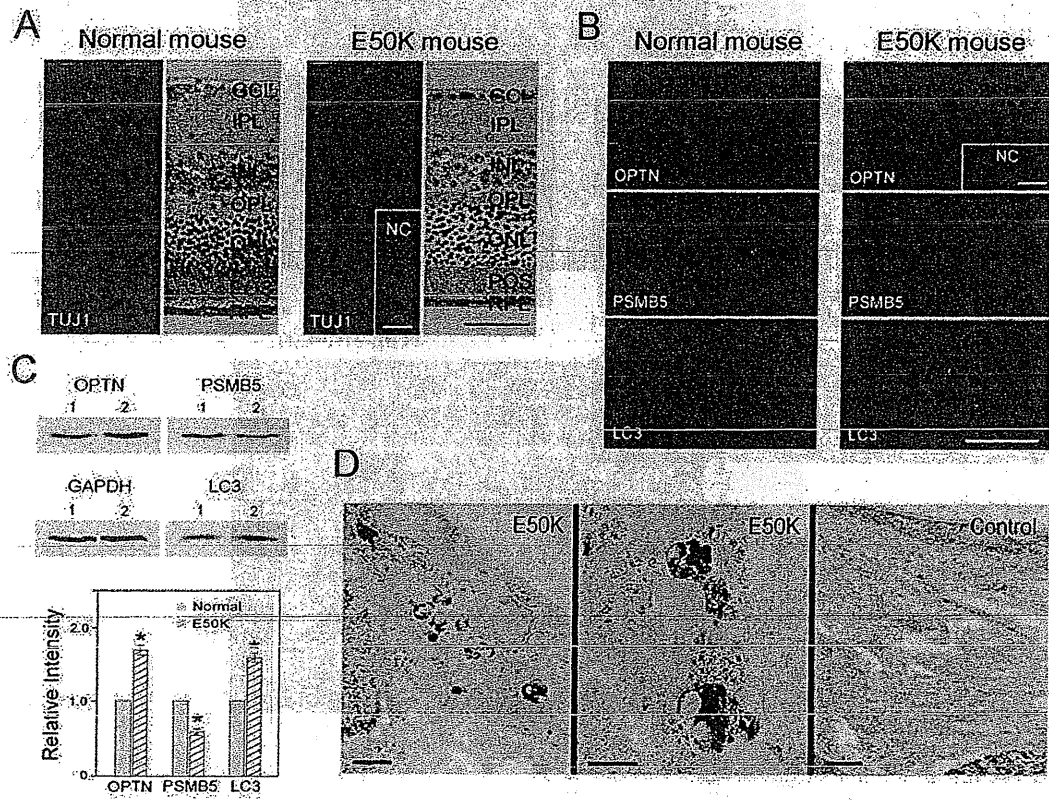


Figure 9

Dominant Mutations in *RP11L1* Are Responsible for Occult Macular Dystrophy

Masakazu Akahori,¹ Kazushige Tsunoda,¹ Yozo Miyake,^{1,2} Yoko Fukuda,³ Hiroyuki Ishiura,³ Shoji Tsuji,³ Tomoaki Usui,⁴ Tetsuhisa Hatase,⁴ Makoto Nakamura,⁵ Hisao Ohde,⁶ Takeshi Itabashi,¹ Haru Okamoto,¹ Yuichiro Takada,¹ and Takeshi Iwata^{1,*}

Occult macular dystrophy (OMD) is an inherited macular dystrophy characterized by progressive loss of macular function but normal ophthalmoscopic appearance. Typical OMD is characterized by a central cone dysfunction leading to a loss of vision despite normal ophthalmoscopic appearance, normal fluorescein angiography, and normal full-field electroretinogram (ERGs), but the amplitudes of the focal macular ERGs and multifocal ERGs are significantly reduced at the central retina. Linkage analysis of two OMD families was performed by the SNP High Throughput Linkage analysis system (SNP HiTLink), localizing the disease locus to chromosome 8p22-p23. Among the 128 genes in the linkage region, 22 genes were expressed in the retina, and four candidate genes were selected. No mutations were found in the first three candidate genes, methionine sulfoxide reductase A (*MSRA*), GATA binding 4 (*GATA4*), and pericentriolar material 1 (*PCMI*). However, amino acid substitution of p.Arg45Trp in retinitis pigmentosa 1-like 1 (*RP11L1*) was found in three OMD families and p.Trp960Arg in a remaining OMD family. These two mutations were detected in all affected individuals but in none of the 876 controls. Immunohistochemistry of *RP11L1* in the retina section of cynomolgus monkey revealed expression in the rod and cone photoreceptor, supporting a role of *RP11L1* in the photoreceptors that, when disrupted by mutation, leads to OMD. Identification of *RP11L1* mutations as causative for OMD has potentially broader implications for understanding the differential cone photoreceptor functions in the fovea and the peripheral retina.

Occult macular dystrophy (OMD) is an autosomal-dominant form of inherited macular dystrophy characterized by progressive decrease of visual acuity due to macular dysfunction, which was first reported by Y.M. et al. in 1989.¹⁻³ The disorder was called "occult" because of the fact that the macular dysfunction of this disease is hidden by a normal fundus appearance. Typical OMD, as described by Y.M. et al., is characterized by central cone dysfunction and in some cases rod dysfunction, leading to a loss of vision despite normal ophthalmoscopic appearance, normal fluorescein angiography, and normal full-field electroretinograms (ERGs). However, the amplitudes of the focal macular ERGs and multifocal ERGs are significantly reduced, indicating dysfunction of the central retina.^{1,2,4} OMD is known for its broad range of age at disease onset, from 6 to 81 yrs. Brockhurst et al. have reported age at onset of four out of eight OMD patients at over 65 yrs⁵ and similar findings have also been observed in earlier cases.^{1,2} The patient III-3 in family 1 did not notice any visual disturbance in her right eye even at the age of 81 yrs.

The four families shown in Figure 1 demonstrate dominant inheritance of the OMD phenotype. None of the patients had ocular diseases other than OMD, except senile cataract or diabetic retinopathy. Control family members were confirmed to be normal via a complete ophthalmic examination including focal macular ERGs or multifocal

ERGs. For this study, the ethics review committees of the National Hospital Organization Tokyo Medical Center, the Niigata University Graduate School of Medical and Dental Sciences, and the Nagoya University Medical School approved the study, and written informed consent was obtained from both affected and unaffected subjects.

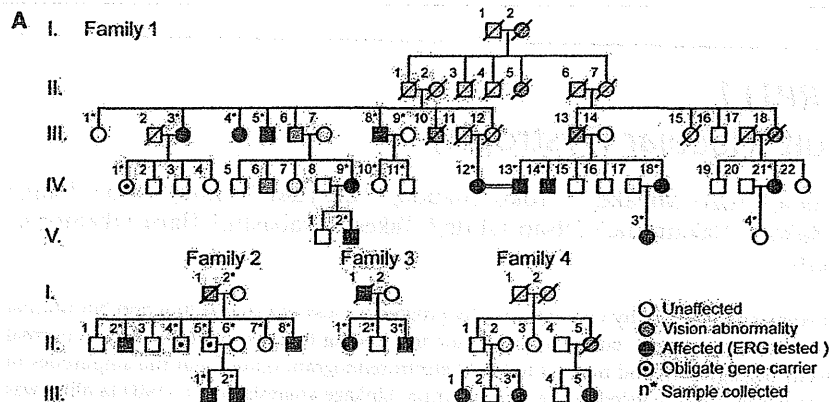
Linkage analysis of OMD families 1 and 2 was performed. Eighteen individuals from family 1 and eleven individuals from family 2 were genotyped by Affymetrix's Genome-Wide Human SNP array 6.0 in accordance with the manufacturer's instructions (Affymetrix, Santa Clara, CA). DNA samples from family 2 were subjected to whole-genome amplification with the use of REPLI-g (QIAGEN, Tokyo, Japan) prior to SNP genotyping. With SNP HiTLink⁶ used as a pipeline, SNPs with a Hardy-Weinberg p value > 0.001 , a call rate of 1, and a maximum confidence score > 0.02 were used for the analysis. SNPs with the minor allele frequency of 0 in controls were eliminated from the analysis. Parametric multipoint linkage analysis (autosomal-dominant model with a setting of liability classes; age-dependent penetrance of 0.19, 0.55, and 0.91 for 0-20, 21-40, and > 41 yrs old, respectively, and disease frequency of 0.000001) was performed with Allegro version 2,⁷ intermarker distance from 80 kb to 120 kb with the use of SNP HiTLink. Because of the limitation of computational capacity, family 1 was divided into two branches (branch 1-1: descendants of II-1; branch

¹National Institute of Sensory Organs, National Hospital Organization Tokyo Medical Center, 2-5-1 Higashigaoka, Meguro-ku, Tokyo 152-8902 Japan;

²Aichi Medical University, 21 Yazakokarimata, Nagakute-cho, Aichi-gun, Aichi-ken, 489-1195 Japan, ³Department of Neurology, Graduate School of Medicine, the University of Tokyo, 7-3-1, Hongo, Bunkyo-ku, Tokyo, 113-8655 Japan; ⁴Division of Ophthalmology and Visual Science, Graduate School of Medical and Dental Sciences, Niigata University, Niigata, 757, Ichibancho, Asahimachidori, Niigata, 951-8510 Japan; ⁵Nakamura Eye Clinic, 107-10, Kisei-cho, Nishi-ku, Nagoya, 452-0816 Japan; ⁶Department of Ophthalmology, School of Medicine, Keio University, 35 Shinanomachi, Shinjuku-ku, Tokyo 160-8582, Japan

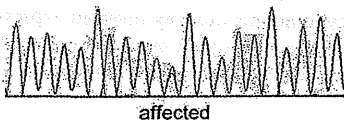
*Correspondence: iwataakeshi@kankakuki.go.jp

DOI 10.1016/j.ajhg.2010.08.009 ©2010 by The American Society of Human Genetics. All rights reserved.

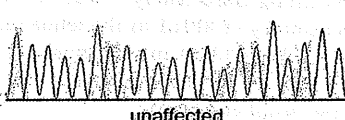


B R45W

G D P R>W F A G
AGGGGATCCAGGGTTTGCTGG

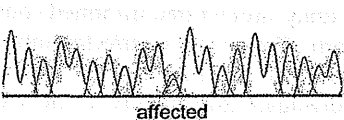


G D P R F A G
AGGGGATCCACGGTTTGCTGG



W960R

V R E W>R L D N
GGTCCGCGAATGGCTGGACAA



V R E W L D N
GGTCCGCGAATGGCTGGACAA



1-2: descendants of II-7) for multipoint linkage analysis. Haplotypes were reconstructed by Allegro.

The parametric linkage study of family 1 using SNP microarrays and SNP HiLink mapped the disease locus to an approximately 10 Mb region of chromosome 8p22-p23 with a maximum LOD score of 3.77 (Figure 2). Parametric linkage analysis of affected individuals only produced similar results (Figure 3 and Figure S2 available online). A common haplotype between rs365309 and rs2632841 was shared by all of the affected individuals (Table 1). With the additional linkage study of family 2, the cumulative parametric multipoint LOD score rose to over 4 (Figure S1). A total of 128 known genes were found within the approximately 10 Mb linkage-associated region, containing 22 retina-expressed genes as candidates for mutational analyses. No mutations were found in the first three candidate genes, methionine sulfoxide reductase A (*MSRA*), GATA binding 4 (*GATA4*), and pericentriolar material 1 (*PCMI*). However, a c.362C>T (p.Arg45Trp) substitution in retinitis pigmentosa 1-like 1 (*RP1L1* [MIM 608581]) was found in all affected individuals in family 1. We further extended the mutational analysis of *RP1L1* to three other families with autosomal OMD, and we identified the p.Arg45Trp alteration in families 2 and 4 and

Figure 1. Autosomal OMD Families and DNA Sequencing of *RP1L1*

(A) The four families shown demonstrate dominant inheritance of the OMD phenotype. In all presented families, none of the patients had ocular diseases other than OMD, except senile cataract and diabetic retinopathy. Control family members were confirmed to be normal via a complete ophthalmic examination including focal macular ERGs or multifocal ERGs. (B) DNA sequencing of both p.Arg45Trp and p.Trp960Arg mutations found in four independent families.

a c.3107T>C (p.Trp960Arg) mutation in family 3 (Table 2). Additionally, known and unknown natural variants were found in *RP1L1*, as shown in Table S2. Unknown SNPs were submitted to the dbSNP database.

In these four families, all of the affected individuals carried one of the two mutations identified in this study, c.362C>T or c.3107T>C. We identified three apparently unaffected individuals carrying the p.Arg45Trp mutation, which suggest a reduced penetrance of the mutation or possibly a later onset of the disease for these individuals. Both mutations were absent in 1752 Japanese control chromosomes.

Immunohistochemistry of *RP1L1* in the macula section of primate *Cynomolgus* monkeys (*Macaca fascicularis*) was performed. The eyes from a 6-yr-old normal male cynomolgus monkey were obtained from Tsukuba Primate Research Center, National Institute of Biomedical Innovation, Japan. All experimental procedures were approved by the Animal Welfare and Animal Care Committee of the National Institute of Biomedical Innovation, in compliance with guidelines of the Association for Research in Vision and Ophthalmology. *Cynomolgus* eyes were removed and immediately fixed overnight with 4% paraformaldehyde in 0.1 M phosphate buffer, pH 7.4. After washing in PBS, eyes were cryoprotected in the gradient sucrose dissolved in PBS and embedded into optimal cutting temperature (OCT) compound (Tissue Tek, Miles, IL, USA). Frozen retinal sections cut at 8 μm thickness with cryostat were incubated at 4°C with a 1:500 dilution of human *RP1L1* polyclonal antibody raised against the N terminus of human *RP1L1* (Santa Cruz Biotechnology, Santa Cruz, CA, USA). Immunofluorescence was visualized with Alexa 568 goat anti-rabbit IgG (Invitrogen, Carlsbad, CA, USA), Alexa 488 PNA (Invitrogen) for detection of cone photoreceptor, and DAPI (Invitrogen) for nuclear staining. Fluorescence images were analyzed with a confocal laser

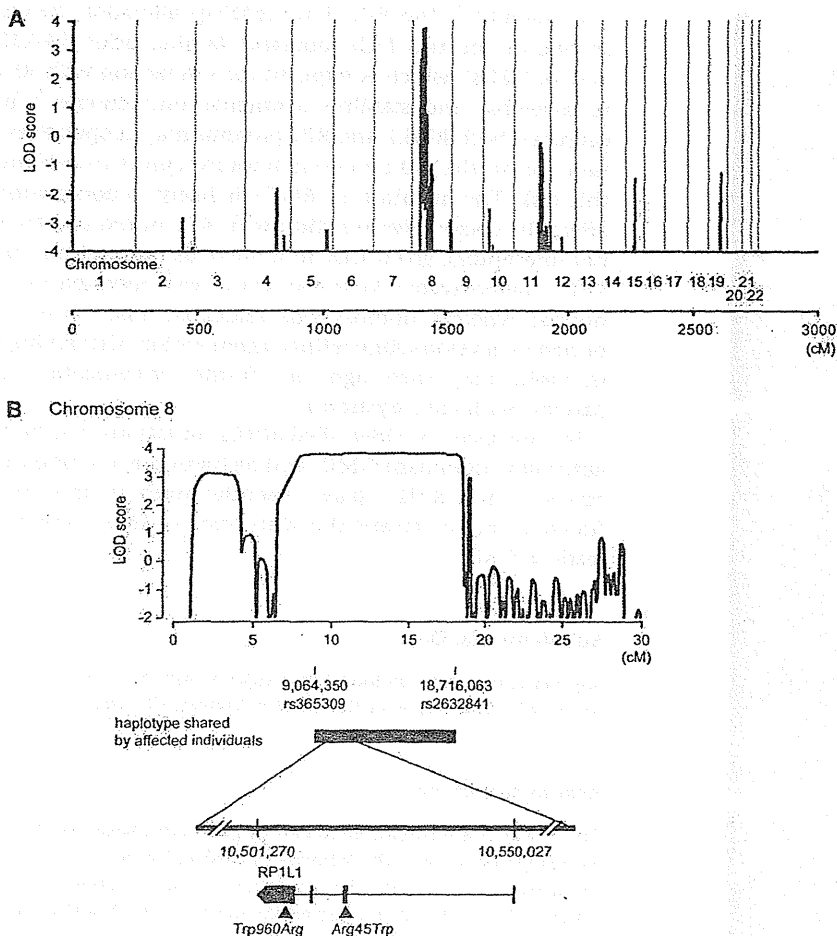


Figure 2. Linkage Analysis and Haplotype Analysis of Family 1

(A) Parametric multipoint linkage analysis of family 1. Horizontal axis indicates cumulative position (cM) from the short arm of chromosome 1. As a result of computational capacity, family 1 was divided into two branches for calculation of LOD scores. No other chromosomes except chromosome 8 yielded a positive LOD score.

(B) Parametric multipoint linkage analysis of family 1 and mutations in *RP1L1*. A maximum LOD score of 3.77 was obtained at 8p32.1-8p22. A haplotype bounded by rs365309 (physical position: 9,064,350 in the hg18 assembly of the UCSC Genome Browser) and rs2632841 (18,716,063) was shared by all affected individuals. Horizontal axis indicates the position (cM) on the short arm of chromosome 8. Vertical axis indicates the parametric multipoint LOD score. Mutations (p.Arg45Trp and p.Trp960Arg) are demonstrated.

patients.^{1,2} It is likely that the initial event may be macular cone specific but may later extend to rod abnormality. Further investigation of *RP1L1* function is required in order to answer these clinical observations.

RP1L1 was originally cloned as a gene derived from common ancestor as retinitis pigmentosa 1 (*RP1* [MIM 180100]) on the same chromosome 8.^{11,12} *RP1L1* shares 35% amino acid

microscope (Radiance 2000, Bio-Rad Laboratories, Hercules, CA, USA).

To our surprise, the immunohistochemistry of *RP1L1* in the macula section of *Cynomolgus* monkeys revealed expression in retinal rod and cone photoreceptors by human *RP1L1* antibody (Figure 3). This expression pattern is significantly different from the previous study of mouse *RP1L1*, in which *RP1L1* was localized exclusively in axoneme of rods.⁸ Furthermore, the human amino acid sequence is only 39% identical to that of the mouse, due to a lack of both polymorphic 16 amino acid repeats or a lack of the highly repetitive Glu-rich region, making mouse *RP1L1* protein considerably shorter than the human protein, which may lead to different functional roles in the primate retina. Recent investigation of photoreceptor structure in OMD patients using advanced optical coherence tomography suggests that the predominant defect involves the cone photoreceptor.^{9,10} Our optical coherence tomography observations also show loss of the cone outer segment tip and irregularity of the inner segment/outer segment junction in the center of the macula of all examined case individuals in family 1 (data not shown). Y.M. et al. have observed that not only cone but also rod sensitivity in the macula was abnormal in some of the older

identity with *RP1*, a gene responsible for 5%–10% of autosomal-dominant retinitis pigmentosa (RP [MIM 268000]) worldwide.^{13–15} When *RP1L1* was first identified, a number of attempts were made to identify mutations in *RP1L1* in various RP patients, with no success. The present study demonstrates that *RP1L1* mutation is responsible for OMD, but not for RP. Patients with RP carrying the most common RP1 alteration, p.Arg677X, exhibit night and peripheral vision disturbance beginning in the third decade of life. RP1 is found exclusively in the retina and is localized to both rods and cones. Rod-cone functional comparison in RP patients has indicated that rod sensitivity loss is at least 2 log units greater than cone sensitivity loss.¹³ Thus phenotypic characteristics of RP caused by *RP1* mutations and those of OMD caused by *RP1L1* mutations perfectly agree with the different localizations of *RP1* and *RP1L1* in retina.

The outer segments of rod and cone photoreceptors are highly specialized cilia containing hundreds of disc membranes stacked in an orderly array along the photoreceptor axoneme. Previous studies have shown that *RP1* is part of the axoneme and is required for this correct orientation and higher-order stacking of outer segment discs.¹⁶ This is achieved by the interaction of *RP1* with the

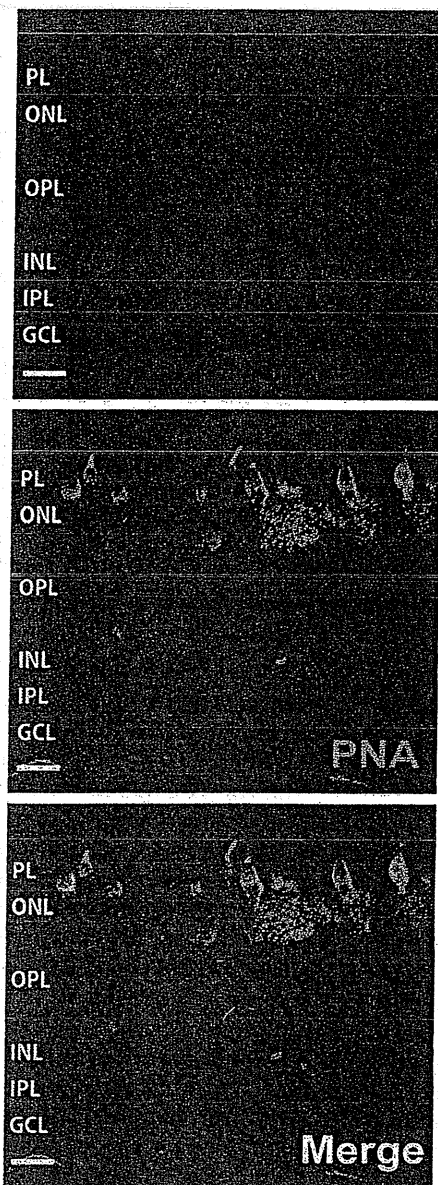


Figure 3. Immunohistochemistry of RP1L1 in the Cynomolgus Monkey Retina

Localization of RP1L1 in the rod and cone photoreceptors in the Cynomolgus monkey (*Macaca fuscicularis*). Retina labeled with anti-human RP1L1 (red, top); same section labeled with retinal cone specific marker, peanut agglutinin lectin (PNA, green, middle); merged image (bottom). Yellow signal present in cone photoreceptor resulted from combination of the red signal of RP1L1 and the green signal of PNA. Cell nuclei were stained with DAPI (blue). PL, photoreceptor layer; ONL, outer nuclear layer; OPL, outer plexiform layer; INL, inner nuclear layer; IPL, inner plexiform layer; GCL, ganglion cell layer. Scale bars represent 20 μ m.

microtubule in the connecting cilia.¹⁷ RP1 contains microtubule-binding domains (amino acids 28–228) of neuronal microtubule-associated protein (MAP) doublecortin (DCX), which is required to maintain axoneme length

and stability.¹⁸ The RP1L1 p.Arg45Trp alteration resides in one of the two DCX domains (amino acids 33–113 and 147–228), which is required for interaction with RP1 to assemble and stabilize axonemal microtubules.⁸ In primates, both RP1L1 and RP1 proteins may cooperatively function in the rod and cone photoreceptors to perform this task. The mutation in *RP1L1* is likely to dominantly affect the cooperative function with RP1 in rod and cone photoreceptors, given that in a previous publication, the *RP1L1* heterozygous knockout mice were reported to be normal whereas homozygous knockout mice were reported to develop subtle retinal degeneration. Our findings in OMD may shed light for further investigation of patients with cone dystrophy.

In conclusion, we identified *RP1L1* mutations that cause autosomal-dominant OMD, and furthermore, our findings revealed that *RP1L1* plays essential roles in the cone functions in human and that disruption of *RP1L1* function leads to OMD.

Supplemental Data

Supplemental Data include three figures and one table can be found with this article online at <http://www.cell.com/AJHG/>.

Acknowledgments

This research was supported in part by grants to Takeshi Iwata and Kazushige Tsunoda by the Ministry of Health, Labour, and Welfare of Japan. This work was also supported in part to Shoji Tsuji by KAKENHI (Grant-in-Aid for Scientific Research) on Priority Areas, Applied Genomics, the Global COE Program, and Scientific Research (A) from the Ministry of Education, Culture, Sports, Science and Technology of Japan.

Received: June 29, 2010

Revised: August 10, 2010

Accepted: August 12, 2010

Published online: September 9, 2010

Web Resources

The URLs for data presented herein are as follows:

dbSNP, www.ncbi.nlm.nih.gov/projects/SNP/

SNP HiTLink software, <http://www.dynacom.co.jp/u-tokyo.ac.jp/snphitlink/>

Accession Numbers

The dbSNP accession numbers for the SNPs reported in this paper are ss252841181 and ss252841182.

References

- Miyake, Y., Ichikawa, K., Shiose, Y., and Kawase, Y. (1989). Hereditary macular dystrophy without visible fundus abnormality. *Am. J. Ophthalmol.* 108, 292–299.

Table 1. Disease-Linked Haplotypes in Families 1 and 2

| Probe Set ID | dbSNP rs ID | Position | Family 1 | | | | | Family 2 | |
|-------------------------|-------------|------------|------------|------|------------|-------|-------|----------|-------|
| | | | Branch 1-1 | | Branch 1-2 | | | II-2 | III-2 |
| | | | III-8 | IV-9 | IV-13 | IV-18 | IV-21 | | |
| SNP_A-8338925 | rs365309 | 9,064,350 | (A) | (A) | A | A | B | A | A |
| SNP_A-8281994 | rs1530483 | 9,065,671 | B | B | B | B | B | B | B |
| SNP_A-8360926 | rs10086673 | 10,342,727 | B | B | (B) | B | B | (A) | A |
| SNP_A-2082488 | rs9329223 | 10,369,164 | A | A | A | A | A | (B) | B |
| SNP_A-2013182 | rs6601491 | 10,453,427 | B | B | B | B | B | (A) | A |
| <i>RP1L1</i> p.Arg45Trp | c.133C>T | 10,517,989 | T | T | T | T | T | T | T |
| SNP_A-8345504 | rs10097570 | 10,586,268 | A | A | A | A | (A) | (B) | B |
| SNP_A-1790165 | rs10111051 | 10,590,882 | A | A | A | A | (A) | (B) | B |
| SNP_A-8587750 | rs2163379 | 10,769,460 | A | A | A | (A) | A | (B) | B |
| SNP_A-8500791 | rs7460507 | 11,006,485 | B | B | B | B | B | A | A |
| SNP_A-8525908 | rs9772321 | 12,536,010 | A | A | A | A | A | A | A |
| SNP_A-8283296 | rs1021087 | 13,500,502 | A | (A) | (A) | A | A | B | B |
| SNP_A-8441723 | rs6987209 | 14,501,302 | B | B | B | B | B | B | B |
| SNP_A-2044287 | rs7818067 | 15,580,087 | A | A | A | A | A | A | A |
| SNP_A-4273924 | rs6992112 | 16,689,526 | A | A | A | A | A | A | (A) |
| SNP_A-8447659 | rs471041 | 17,707,836 | B | B | B | B | B | B | B |
| SNP_A-8399664 | rs2638658 | 18,713,620 | A | (A) | (A) | A | A | (B) | B |
| SNP_A-4233785 | rs2632841 | 18,716,063 | B | B | (B) | B | A | B | B |

Disease-linked haplotypes of the two patients (IV-9 and III-8) who are descendants from II-1 (branch 1-1 of family 1), the three patients (IV-13, IV-18, and IV-21) who are descendants from II-7 (branch 1-2 of family 1), and the two patients (II-2 and III-2) from family 2 are shown. Haplotypes are unequivocally determined, except those with brackets that are inferred to minimize the number of recombination events. Disease-linked haplotypes of the two branches of family 1 are the same, confirming that all affected individuals in family 1 share the same haplotype. Recombination events in the family was observed at rs365309 (telomeric boundary) and at rs2632841 (centromeric boundary). When disease haplotypes are compared between families 1 and 2, who share the p.Arg45Trp mutation in *RP1L1* in common, disease-linked haplotypes flanking the *RP1L1* locus are different between these families, suggesting that the p.Arg45Trp mutation originated independently.

- Miyake, Y., Horiguchi, M., Tomita, N., Kondo, M., Tanikawa, A., Takahashi, H., Suzuki, S., and Terasaki, H. (1996). Occult macular dystrophy. *Am. J. Ophthalmol.* 122, 644–653.
- Wildberger, H., Niemeyer, G., and Junghardt, A. (2003). Multifocal electroretinogram (mfERG) in a family with occult macular dystrophy (OMD). *Klin. Monatsbl. Augenheilkd.* 220, 111–115.
- Piao, C.H., Kondo, M., Tanikawa, A., Terasaki, H., and Miyake, Y. (2000). Multifocal electroretinogram in occult macular dystrophy. *Invest. Ophthalmol. Vis. Sci.* 41, 513–517.
- Brockhurst, R.J., and Sandberg, M.A. (2007). Optical coherence tomography findings in occult macular dystrophy. *Am. J. Ophthalmol.* 143, 516–518.
- Fukuda, Y., Nakahara, Y., Date, H., Takahashi, Y., Goto, J., Miyashita, A., Kuwano, R., Adachi, H., Nakamura, E., and Tsuji, S. (2009). SNP HiTLink: a high-throughput linkage analysis system employing dense SNP data. *BMC Bioinformatics* 10, 121.
- Gudbjartsson, D.F., Thorvaldsson, T., Kong, A., Gunnarsson, G., and Ingólfssdóttir, A. (2005). Allegro version 2. *Nat. Genet.* 37, 1015–1016.
- Yamashita, T., Liu, J., Gao, J., LeNoue, S., Wang, C., Kaminoh, J., Bowne, S.J., Sullivan, L.S., Daiger, S.P., Zhang, K., et al. (2009). Essential and synergistic roles of RP1 and RP1L1 in rod photoreceptor axoneme and retinitis pigmentosa. *J. Neurosci.* 29, 9748–9760.
- Park, S.J., Woo, S.J., Park, K.H., Hwang, J.M., and Chung, H. (2010). Morphologic photoreceptor abnormality in occult macular dystrophy on spectral-domain optical coherence tomography. *Invest. Ophthalmol. Vis. Sci.* 51, 3673–3679.
- Sisk, R.A., Berrocal, A.M., and Lam, B.L. (2010). Loss of foveal cone photoreceptor outer segments in occult macular dystrophy. *Ophthalmic Surg Lasers Imaging* 41, 1–3.
- Conte, I., Lestingi, M., den Hollander, A., Alfano, G., Ziviello, C., Pugliese, M., Circolo, D., Caccioppoli, C., Ciccodicola, A., and Banfi, S. (2003). Identification and characterization of the retinitis pigmentosa 1-like1 gene (*RP1L1*): a novel candidate for retinal degenerations. *Eur. J. Hum. Genet.* 11, 155–162.
- Bowne, S.J., Daiger, S.P., Malone, K.A., Heckenlively, J.R., Kennan, A., Humphries, P., Hughbanks-Wheaton, D., Birch, D.G., Liu, Q., Pierce, E.A., et al. (2003). Characterization of

Table 2. Summary of RP1L1 Mutations in Families with OMD

| ID in Pedigree | Clinical Stage | Sex | Age at Diagnosis | Age at Onset in Estimation | Mutation | Best Corrected Visual Acuity (Right / Left) |
|----------------|----------------|-----|------------------|----------------------------|-----------|---|
| 1 III3 | affected | F | 81 | 50 | c.362C>T | 1.2 / 0.1 |
| 1 III4 | affected | F | 71 | 25 | c.362C>T | 0.4 / 0.5 |
| 1 III5 | affected | M | 74 | 30 | c.362C>T | 0.2 / 0.3 |
| 1 III8 | affected | M | 82 | 20 | c.362C>T | 0.2 / 0.2 |
| 1 IV1 | unaffected | F | 60 | - | c.362C>T | 1.2 / 1.2 |
| 1 IV9 | affected | F | 49 | unknown | c.362C>T | 1.2 / 1.2 |
| 1 IV12 | affected | F | 69 | 50 | c.362C>T | 0.1 / 0.07 |
| 1 IV13 | affected | M | 70 | 20 | c.362C>T | 0.1 / 0.1 |
| 1 IV14 | affected | M | 66 | 30 | c.362C>T | 0.2 / 0.3 |
| 1 IV18 | affected | F | 58 | 12 | c.362C>T | 0.1 / 0.1 |
| 1 IV21 | affected | F | 58 | 47 | c.362C>T | 0.1 / 0.4 |
| 1 V2 | affected | M | 20 | 13 | c.362C>T | 0.3 / 0.3 |
| 1 V3 | affected | F | 19 | 6 | c.362C>T | 0.2 / 0.15 |
| 2 II2 | affected | M | 69 | unknown | c.362C>T | 0.2 / 0.2 |
| 2 II4 | unaffected | M | 58 | - | c.362C>T | 1.0 / 1.0 |
| 2 II5 | unaffected | M | 55 | - | c.362C>T | 1.0 / 1.0 |
| 2 II8 | affected | M | 52 | unknown | c.362C>T | 0.2 / 0.3 |
| 2 III1 | affected | M | 23 | 23 | c.362C>T | 0.2 / 0.3 |
| 2 III2 | affected | M | 20 | 20 | c.362C>T | 0.3 / 0.3 |
| 3 III1 | affected | F | 29 | 12 | c.3107T>C | 0.2 / 0.2 |
| 3 III3 | affected | M | 19 | 13 | c.3107T>C | 0.2 / 0.3 |
| 4 III3 | affected | F | 52 | 30 | c.362C>T | 0.15 / 0.15 |

Summary of individuals from autosomal OMD families 1–4, in whom p.Arg45Trp or p.Trp960Arg mutations of *RP1L1* were found. Three unaffected individuals at the age of 55–60 were found with the mutation. These individuals suggest a reduced penetrance of the mutation or a possible onset at a later age.

RP1L1, a highly polymorphic paralog of the retinitis pigmentosa 1 (RP1) gene. *Mol. Vis.* 9, 129–137.

- Pierce, E.A., Quinn, T., Meehan, T., McGee, T.L., Berson, E.L., and Dryja, T.P. (1999). Mutations in a gene encoding a new oxygen-regulated photoreceptor protein cause dominant retinitis pigmentosa. *Nat. Genet.* 22, 248–254.
- Sullivan, L.S., Heckenlively, J.R., Bowne, S.J., Zuo, J., Hide, W.A., Gal, A., Denton, M., Inglehearn, C.F., Blanton, S.H., and Daiger, S.P. (1999). Mutations in a novel retina-specific gene cause autosomal dominant retinitis pigmentosa. *Nat. Genet.* 22, 255–259.
- Jacobson, S.G., Cideciyan, A.V., Iannaccone, A., Weleber, R.G., Fishman, G.A., Maguire, A.M., Affatigato, L.M., Bennett, J., Pierce, E.A., Danciger, M., et al. (2000). Disease expression of RP1 mutations causing autosomal dominant retinitis pigmentosa. *Invest. Ophthalmol. Vis. Sci.* 41, 1898–1908.
- Liu, Q., Lyubarsky, A., Skalet, J.H., Pugh, E.N., Jr., and Pierce, E.A. (2003). RP1 is required for the correct stacking of outer segment discs. *Invest. Ophthalmol. Vis. Sci.* 44, 4171–4183.
- Liu, Q., Zuo, J., and Pierce, E.A. (2004). The retinitis pigmentosa 1 protein is a photoreceptor microtubule-associated protein. *J. Neurosci.* 24, 6427–6436.
- Gleeson, J.G., Allen, K.M., Fox, J.W., Lamperti, E.D., Berkovic, S., Scheffer, I., Cooper, E.C., Dobyns, W.B., Minnerath, S.R., Ross, M.E., and Walsh, C.A. (1998). Doublecortin, a brain-specific gene mutated in human X-linked lissencephaly and double cortex syndrome, encodes a putative signaling protein. *Cell* 92, 63–72.

The American Journal of Human Genetics, Volume 87

Supplemental Data

Dominant Mutations in *RP1L1*

Are Responsible for Occult Macular Dystrophy

Masakazu Akahori, Kazushige Tsunoda, Yozo Miyake, Yoko Fukuda, Hiroyuki Ishiura, Shoji Tsuji, Tomoaki Usui, Tetsuhisa Hatase, Makoto Nakamura, Hisao Ohde, Takeshi Itabashi, Haru Okamoto, Yuichiro Takada, and Takeshi Iwata